

# Formation of turbid ice during autumn freeze-up in the Kara Sea

Lars H. Smedsrud



A one-dimensional (vertical) model is used to estimate the mass of ice-rafted sediment in turbid sea ice on the shallow Kara Sea shelf during autumn freeze-up. Sediment is entrained into the ice through aggregation with frazil ice crystals that are diffused downwards by wind-generated turbulence. Data from local meteorological stations are used to force the model, while water stratification and sediment concentrations from the area are used to initiate the model. Model results indicate a 0.2 m thick layer of slush ice created during 48 h with a mean wind of 6 m/s and an air temperature of  $-10^{\circ}\text{C}$ . This ice contains ca. 20 mg/l of sediment, or in total ca. 2% of the annual sediment discharge by nearby rivers. In shallow areas ( $<20$  m depth) the process is very effective with winds of ca. 12 m/s, and the process can incorporate many years of sediment discharge. In the deeper areas ( $>20$  m depth), the strong salinity stratification implies that winds above 18 m/s are needed for the process to be effective. For the rest of the winter months the same process may lead to additional sediment incorporated in a coastal polynya, but the freeze-up alone has the capacity to incorporate the total summer discharge of sediment into the surface ice. Calculated sediment concentrations in the surface ice cover are in the range 3 mg/l-19 g/l, in good agreement with available field data.

*L. H. Smedsrud, Geophysical Institute, Allègaten 70, University of Bergen, NO-5007 Bergen, Norway, larsh@gfi.uib.no.*

The Arctic Ocean is surrounded by shallow seas which are nearly ice-free in the summer and ice-covered during the long winter. Some time during September–October the upper mixed layer reaches its freezing point and the falling snow, or frozen sea spray, initiates the formation of the sea ice cover. If conditions are calm during the autumn freeze-up, the sea ice crystals will grow downwards to form a uniform sheet of congelation ice. In contrast, a turbulent freeze-up will form free-floating frazil ice crystals, which are likely to collide with, and aggregate to, sediment in suspension (Smedsrud 2001). This results in turbid ice: granular sea ice with the ice-rafted sediment (IRS) widely distributed throughout the ice (Kempema et al. 1989). Such ice has been sampled in the Laptev, Beaufort and Kara seas

(Osterkamp 1984; Nürnberg 1994; Smedsrud & Eicken 2003).

This study considers the formation of turbid ice in the Kara Sea, which has a wide shelf—about 220 km, with large areas shallower than 60 m. Sediment enters from the Ob and Yenisey rivers and is introduced from coastal and shore-face erosion. The Ob and Yenisey rivers discharge massive quantities of sediment which may carry bonded pollutants, including heavy metals, organochlorines and radionuclide contaminants. If this sediment is incorporated into sea ice and the sea ice becomes second-year ice, the sediment may be transported to the Barents Sea or Fram Strait. Here sea ice melts rapidly, releasing the sediment and bonded pollutants.

Based on topography, six different areas of the

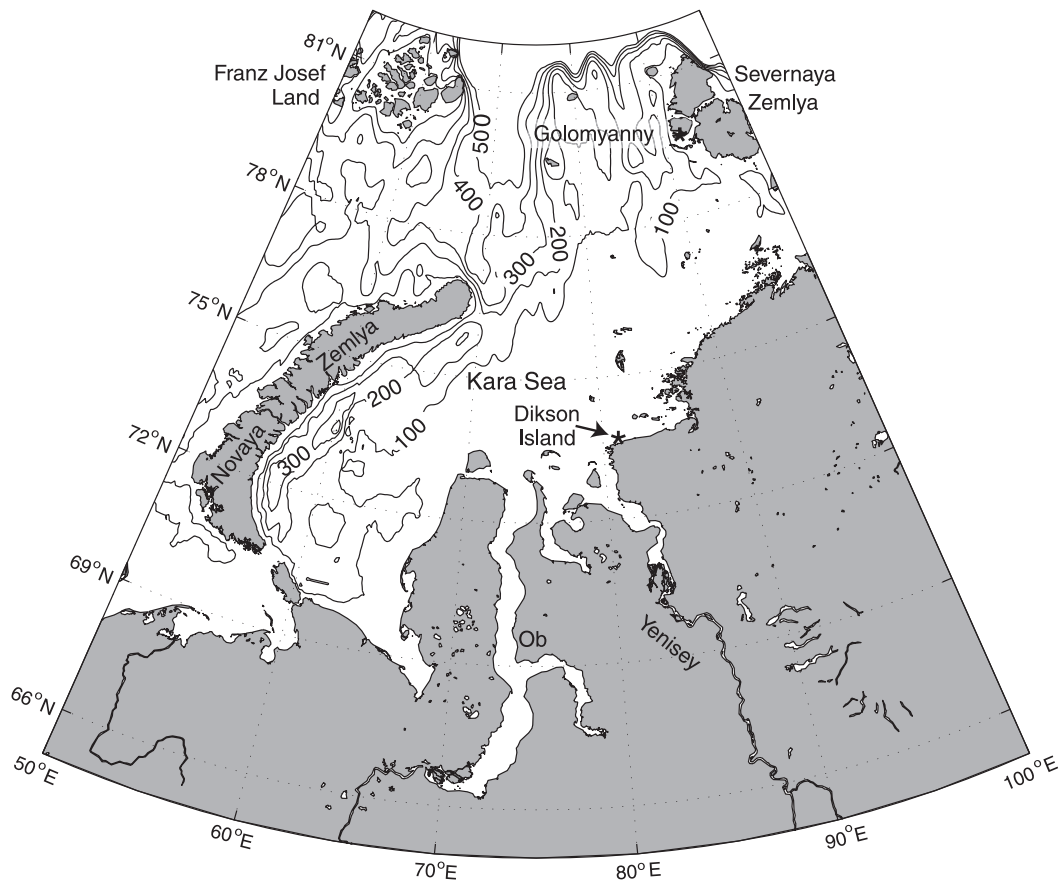


Fig. 1. Map of the Kara Sea and surrounding islands. The meteorological stations at Dikson and Golomyanny islands are indicated with asterisks.

Kara Shelf (here defined as the area with depths less than 100 m, 70–100°E; Fig. 1) are selected, and typical vertical stratifications (salinity profiles) are then chosen, based on available CTD data. The river inflow and sediment processes on the Kara Shelf which initialize the model runs are discussed. The atmospheric forcing—wind, snow and air temperature—is presented and this forms the forcing for the vertical frazil and sediment model: Frasemo (Smedsrud 2002). Sensitivity tests towards different forcing, discussion of model limitations and comparison of results with available field data comprise the last part of the paper.

## Kara Sea background

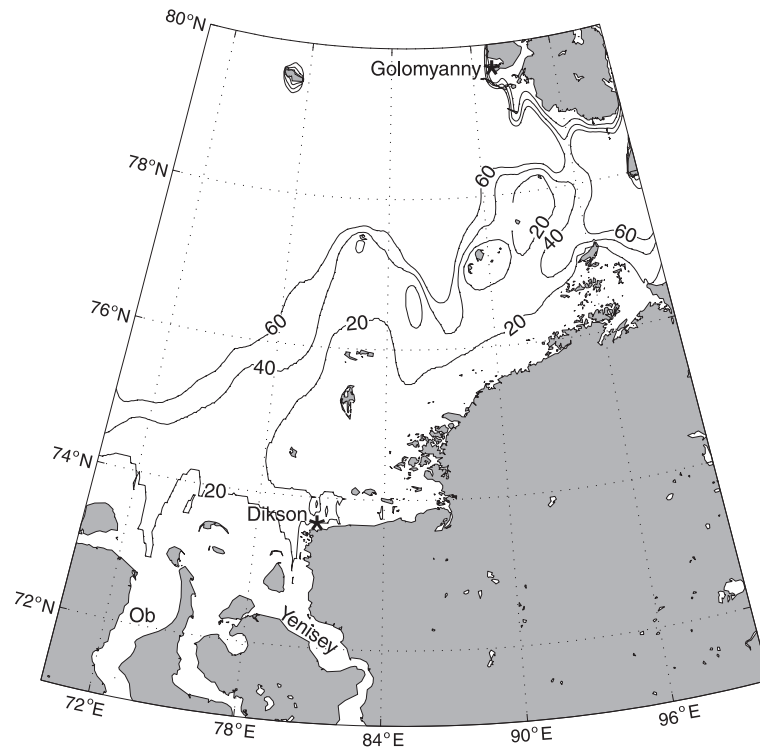
In shallow shelf seas such as the Kara Sea there is

a considerable interannual and seasonal variation in climatic forcing. In the Kara Sea, confidence in observational data is further reduced by the sparseness of the observations, which are often of short duration. There is considerable variation in hydrography (Pavlov & Pfirman 1995), especially in the shallow regions most important for the sediment entrainment processes.

The ice cover of the Kara Sea has rarely been sampled. This is because most cruises to the area have taken place in August–September, when the sea is generally not covered by ice and is easily accessed. Monthly mean sea ice concentration from SMMR data is about 50% for the Kara Shelf in October and 80–90% in November. From December to May ice concentrations are 90–100% all over the Kara Sea (Gloersen et al. 1992).

The mean seasonal hydrography and circula-

Fig. 2. Bathymetry of the Kara Shelf (ETOPO 5 data).



tion was modelled by Harms & Karcher (1999), showing satisfactory results for the hydrography and currents on the shelf. Modelled surface currents are generally north-eastward, driven by the wind fields and steered by topography. The river water flows more or less directly along the Siberian coast as a strong surface current (ca. 10 cm/s) which leaves through Vilkitsky Strait, between Severnaya Zemlya and the mainland. In summer, after the sea ice has melted, the wind forces some of the river water out into the central Kara Sea. Below the surface current (25-50 m depth) is a counter current flowing towards the estuaries in a southward direction all year.

Atlantic water enters the Kara Sea from the north, in the deep trough just east of Franz Josef Land, with a core of 1.5°C and 34.94 psu at 300 m depth. This water, considered a response to the northward flowing surface water, flows southwards and rises until it comes within reach of surface driven mixing (Hanzlick & Aagaard 1980).

This general picture is confirmed by current observations (Johnson et al. 1997). Subtidal variability is high. Many current meters frequently show averaged values of 20 cm/s for 12.5 h blocks. Directions are mostly northwards in the

surface layer. The subtidal variability north of the estuaries correlates well with the local wind, so the winds can play a strong role in spreading the river waters toward the north-west (Johnson et al. 1997).

The Kara Sea is dominated by semi-diurnal tidal oscillations. About 150 km north of the estuaries semi-diurnal currents exceed 50 cm/s (Johnson et al. 1997). For the same rig the mean current speed was only 3 cm/s in the north-west direction (11 day long record). The high tidal amplitude may be partially explained by co-oscillating tides at the mouths of the estuaries. Tidal currents are generally in the range 10-25 cm/s (Kowalik & Proshutinsky 1994).

### Topography

The bathymetry of the shallow Kara Sea shelf is not known in detail. The ETOPO 5 global data base has been used in Fig. 2 and 5 data differ significantly from specific depths at stations in Nygaard (1995), but the average values over the wide shelf should be correct. The discussion of the shelf processes is limited to depths down to 60 m. This makes the total area of the shelf

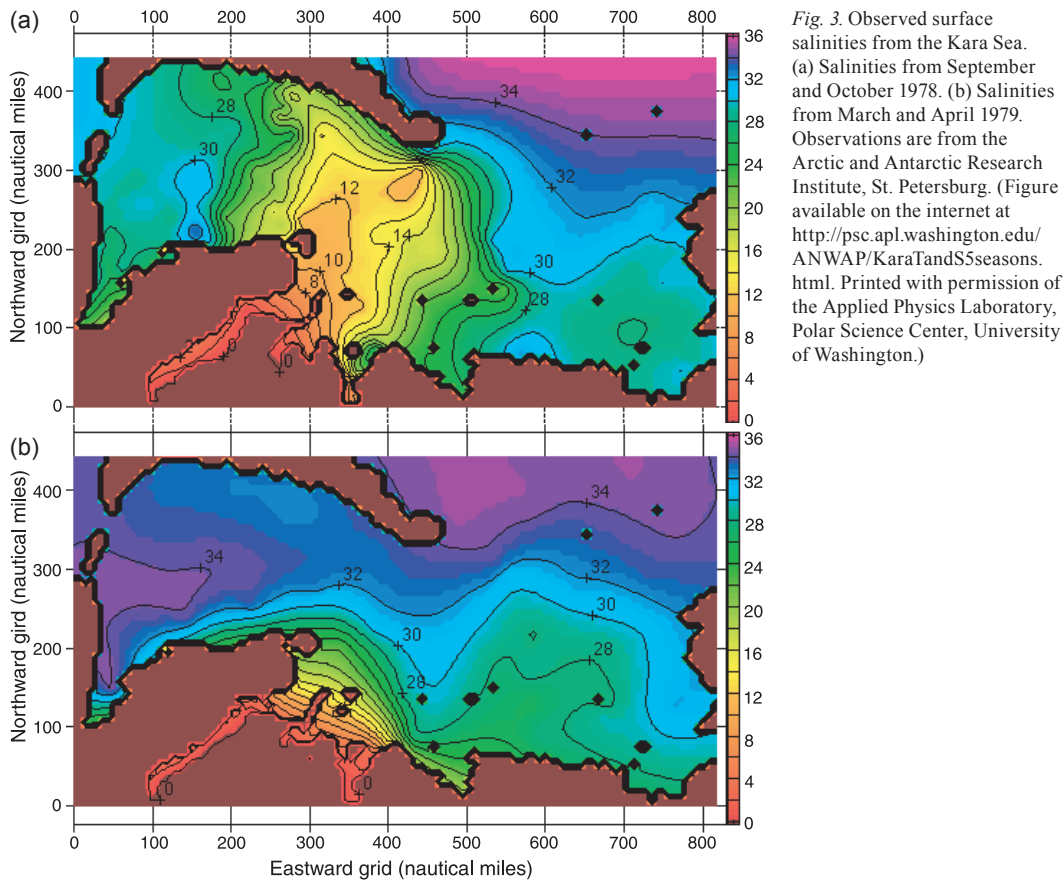


Fig. 3. Observed surface salinities from the Kara Sea. (a) Salinities from September and October 1978. (b) Salinities from March and April 1979. Observations are from the Arctic and Antarctic Research Institute, St. Petersburg. (Figure available on the internet at <http://psc.apl.washington.edu/ANWAP/KaraTandS5seasons.html>. Printed with permission of the Applied Physics Laboratory, Polar Science Center, University of Washington.)

between the Ob estuary and Severnaya Zemlya ca. 216 850 km<sup>2</sup>. Three areas represented by their average depth are delineated to limit the model results and discussions of sensitivity: 0-20 m, 20-40 m and 40-60 m. The area with an average of 10 m depth is 118 035 km<sup>2</sup>, the 30 m average depth area is 67 710 km<sup>2</sup>, and 50 m average depth is 31 110 km<sup>2</sup>.

### Stratification

Vertical density stratification is controlled mostly by salinity, which in turn is mostly governed by the river inflow. The Coriolis Effect makes much of the fresh water follow the coast eastwards from the estuaries as a coastal current, gradually mixing with saltier water along the way. Prevailing winds from the north to north-east during the summer may lead to a spreading of the mixed layer and the river water northwards through Ekman transport (Fig. 3a). As winds vary, the

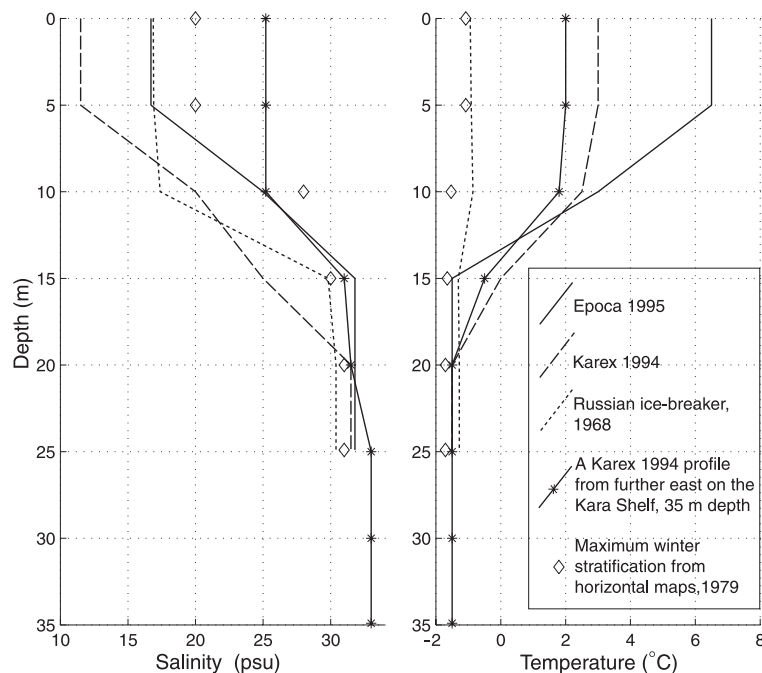
spreading of river water may vary considerably from year to year.

Figure 3a shows the general picture from recent cruises: there is a region outside the Ob and Yenisey estuaries (around 90 km, or 50 nautical miles) with a surface salinity of less than 10 psu.

The focus here is the autumn freeze-up in October, when the river discharge has virtually ceased, so the winter situation is also relevant (Fig. 3b). These are the only available winter data, together with comparable maps from the same months in 1978 and 1980. In these two years the low salinity surface water was confined closer to the coast than in 1979.

In winter, surface salinities have increased to above 20 psu outside the estuaries, whereas in the region to the east salinities are between 26 and 30 psu, close to values in summer. Values at the sea floor are close to 33 psu in winter as well, so the vertical gradients are less than 10 psu outside the estuaries, and between 3-5 psu east of 400

Fig. 4. Vertical temperature and salinity from chosen profiles outside the Ob and Yenisey estuaries on the Kara Sea Shelf. Karex 94 data from Nygaard (1995); EPOCA 1995 data from Krosshavn et al. (1997); Russian ice-breaker data from Sherwood (2000).



nautical miles in Fig. 3. However, there is no indication that the water column becomes vertically homogeneous in shallow water during the winter. This could happen due to the salt released by the sea ice growth, but is opposed by the continuous outflow of river water. Calculated freezing rates are 4-6 m/year (Harms & Karcher 1999).

Two different areas have been selected for the model. The most stratified area, outside the estuaries and with surface salinities between 12 and 18 psu in the autumn (Fig. 3a), will hereafter be referred to as “Area E”. The other area further to the east on the shelf, with surface salinities between 26 and 30 psu, is henceforth “Area S”. The regions between these two have stratifications somewhere in between. Examples of vertical temperature and salinity profiles in the two areas are shown in Fig. 4.

The stratification in salinity in summer for Area E falls within the two measured profiles from 1994 and 1995 (Fig. 4). These stations, about 70 km apart, were obtained in September, indicate some of the year-to-year variability found in Area E. In winter stratification is less, as indicated in Fig. 3b. All surface values are above 20 psu. The lowest salinities (maximum stratification) are shown in Fig. 4. The northernmost portion of Area E has winter surface salinities of

about 33 psu and therefore no stratification, but this is depths greater than 100 m.

Area S has less stratification, comparable to the station at 35 m depth shown in Fig. 4. In summer the upper mixed layer is about 10 m close to the coast, increasing off the coast (Nygaard 1995). From 10 m and downwards, the stratification close to the coast is similar to that of Area E, but the northern portions in deeper water have values which are 1-2 psu higher.

The summer and winter surface salinities (5 m depth) in Area S are similar (Fig. 3). In fact, the winter waters are slightly fresher than in summer. This might be due to the ice cover, which to some extent prohibits wind induced mixing and spreading of the diluted river water. The fast ice edge cuts through Area S, but its position varies from year to year, from about 50 to 180 km off the coast (Dmitrenko et al. 1998). The maximum fast ice edge corresponds closely to the 20 m isobath in Fig. 2. Winter stratification in Area S is close to that of the summer. The maximum stratification is the same, but there is no distinct upper layer, and the salinity increases steadily downwards.

Surface temperatures in Area E are up to 6°C in summer. Below the well mixed surface layer, an intermediate warm layer can be found (Dmitrenko et al. 1998). This layer forms due to

the overlying fresh river water and can persist until ice formation starts. The layer may minimize formation of fast ice in years when the river water stays close to the coast. Such a layer was not evident in the profiles shown in Fig. 4.

Temperatures in the lower layers during summer are generally 0.1–0.3 °C above the in situ freezing point ( $T_f$ ). For a salinity of 32.0 psu,  $T_f$  is –1.75 °C. Observed temperatures normally fall in the range –1.3 to –1.5 °C. In winter the temperature on the Kara Shelf is close to the freezing point at all depths. The station from 1968 shown in Fig. 4 indicates that the upper layer is cooled to the freezing point already in October.

Based on topography and stratification, six different typical classes of stratification have been chosen for model initialization (Table 1). Each class has an upper and lower mixed layer, representing averages over their depths. Upper layer salinities are generally higher than the summer surface values in Area E but are much lower than in winter (Fig. 3). This is an attempt to represent the stratification in late October, also adjusting for the sections from the 1990s. Upper layer salinities in Area S are slightly lower than given in Fig. 3a because more river water was observed in this area in the 1990s. Between the layers salinity is taken to vary linearly. As a simplification, the temperatures of the water columns are set to the in situ freezing point.

#### *River inflow and sediment*

The maximum river outflow to the Kara Sea occurs in June, with ca. 0.14 Sv ( $10^6 \text{ m}^3/\text{s}$ ) (Pavlov & Pfirman 1995). This is about twice as much as in July and August and four times as much as in May, September and October. The rest of the year has a close to constant outflow of 0.01 Sv. Runoff anomalies persist for several years but the aver-

age value used in Harms & Karcher (1999)—0.03 Sv—is identical with the average of the years 1936–1964 (Hanzlick & Aagaard 1980). The range given is 0.023 to 0.04 Sv.

The Kara Sea rivers (Ob, Pur, Taz, Yenisey and Pjasina), and the Lena which empties into the Laptev Sea, have quite low sediment loads compared to other major rivers. Together they drain close to 10% of the total world land area draining into oceans but contribute less than 1% of the total sediment discharge. This is because they drain low-lying (low relief) terrain, portions of which have been stripped of sediment by glaciers (Milliman & Meade 1983).

The Ob and Yenisey rivers have average sediment loads of 41.5 mg/l and 23.2 mg/l, respectively, which makes a total of  $29 \times 10^6$  tonnes per year. This is close to one third of the total calculated sediment discharge to the Arctic Ocean from the Eurasian Arctic (Milliman & Meade 1983). The average level of suspended particulate matter (SPM) in the offshore area was found to be as low as 1.3 mg/l in August and September 1994 (Evenset et al. 1999). For eight stations on the shelf in August and September 1995, with a mean depth of 31.5 m, values are 1.04 mg/l in the surface and 6.08 mg/l in the bottom layer (EPOCA 95, J. Carroll, pers. comm.). The measurements were taken during calm atmospheric conditions.

Average SPM in the estuaries during August and September are much higher than on the shelves: 3.7 mg/l in the Yenisey and 18.8 mg/l in the Ob (Evenset et al. 1999). This confirms that despite its smaller discharge the Ob supplies more sediment than the Yenisey. Values are lower than the annual average and indicate that the major sediment volume probably discharges during the flood in June.

The major sediment loads enter the Kara Sea when there is no ice growth. This means that even if some of these sediments are flushed onto the river ice or sea ice, this ice will melt not far from the river estuary. Undoubtedly, most of the sediment load will end up somewhere on the sea floor of the shelf, be resuspended during high turbulence events, and settle in quiet areas when conditions allow.

The low levels of SPM make it difficult to do grain size analyses on the sediment, so the size distribution of the bottom samples is important information. More than 50% of the bottom sediment is generally silts or clay ( $2 r_s < 63 \mu\text{m}$ ), but variations are high. Some stations have values as

Table 1. Typical and simplified water columns on the Kara Shelf.

	E 10m	E 30m	E 50m	S 10m	S 30m	S 50m
Upper layer						
m	0-4	0-8	0-15	0-4	0-10	0-20
Salinity (psu)	12.0	17.7	20.0	20.0	25.0	28.0
Lower layer						
m	6-10	14-30	20-50	6-10	20-30	30-50
Salinity (psu)	20	31.6	33.0	25.0	33.0	33.0

high as 97% and a few shallow stations (12–17 m) have values around 5%. Grain size distribution varies little down core. Figure 5 shows a surface sample where 79% of the particles are smaller than 63  $\mu\text{m}$  and the median diameter is close to 25  $\mu\text{m}$ . Modern sediment accumulation rates in the estuaries and on the Kara Shelf are ca. 0.1 cm/yr (Evenset et al. 1999). This is much lower than the flux from the rivers. The rest of the sediment must be transported out of the area either as SPM or IRS.

The initial sediment concentrations used are means from the shelf stations during EPOCA 95 (Krosshavn et al. 1997). In Area E the means of three stations were 2.0 mg/l in the upper layer and 8.9 mg/l in the lower. In Area S values are lower: 0.7 mg/l in the upper layer and 4.4 mg/l in the lower (5 stations). Depths were 20–54 m.

#### *Atmospheric forcing*

Air temperatures ( $T_a$ ) and winds are of great importance when ice formation starts in the Kara Sea. Together they allow us to estimate the heat flux from the water to the air, which is directly proportional to the volume of ice produced in a given area. The wind also controls the advection of ice. With southerly winds the newly grown ice will be advected northwards, leaving a polynya between the moving sea ice pack and the coast (or the fast ice edge).

When the mixed surface layer is cooled slightly below the freezing point, frazil ice will start to form at the surface. The subsequent evolution of crystal growth, supercooling and turbulent diffusion of ice crystals in the model is described in the section which presents the model results, based on the atmospheric forcing.

Precipitation is also an important parameter. Monthly mean climatological data show a considerable range in air temperature over the Kara Sea, from +5°C in the south-western parts in August to –33°C over eastern parts in January. Wind fields show strong monsoon-like variabilities due to the seasonal air pressure distribution over the Arctic. From October to March strong stable winds prevail (maximum 8.5 m/s in February), with the wind mainly coming from the south and south-west (Harms & Karcher 1999). Mean speeds in summer are lower (2–4 m/s) and more variable in direction, but northerly to north-easterly winds dominate.

In the absence of very strong and steady cur-

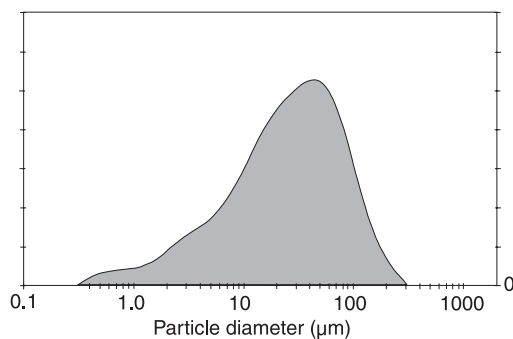


Fig. 5. Size distribution of surface sediment outside the Kara Sea estuaries at 30 m depth (73°23'N, 73°E). Median size is 25  $\mu\text{m}$ . (Figure used with permission of J. Carroll, unpubl. data; see also Carroll & Harms 1999; Carroll et al. 1999.)

rents on continental shelves, the sediment dispersal is mainly controlled by tidal currents or seasonal fluctuations in wave and current intensity. Maximum sediment transport typically accompanies storm activity (Reading 1996). Even if the tidal currents are relatively strong in the Kara Sea (10–25 cm/s, with up to about 50 cm/s near the Ob estuary), tidal currents need to be much stronger to dominate sedimentation processes (Reading 1996). Wind forcing is therefore important, together with a good estimate of the frequency of storms, from the longest data records available. Storm processes are also known to enhance or overprint sediment transport associated with most of the fair-weather processes (Reading 1996).

A data base from the period 1951–1992, including seven meteorological stations around the Kara Sea, is used to estimate the range in conditions during the autumn freeze-up. The data base utilizes records kept at the Arctic and Antarctic Research Institute in St. Petersburg and what has previously been published in the Russian literature (Alexandrov et al. 2000). The meteorological stations at Dikson and Golomyanny islands (Figs. 1, 2) are the ones closest to the Kara Shelf.

Table 2 contains parameters relevant to the freeze-up study, and includes the mean monthly air temperature ( $T_a$ ), the maximum and minimum temperature of the record, mean precipitation during one month, wind speed means, maximum observed instantaneous wind speed during the given month, and average number of days per month with wind stronger than 15 m/s (gale days).

The minimum temperature at Golomyanny is

below zero at least one day per month throughout the year (Alexandrov et al. 2000). At Dikson the average first day of frost is 2 September, ranging from 12 August to 4 October. Based on data from the years 1936–1965, there is a statistical probability of 95% that the maximum wind speed at Dikson is 39 m/s during one year, 46 m/s during five years, 49 m/s during 10 years and 52 m/s during 20 years (Alexandrov et al. 2000).

The data base described above is compared to observations of wind and air temperature from Dikson in the period 1936–1990 from the All-Russian Research Institute of Hydro Meteorological Information—World Data Centre. Data are 6 hourly in the years 1936–1965 and 3 hourly in the years 1966–1990. These data confirm that storms (wind speed >25 m/s) occur 2–4 times a year. Hurricanes (wind speed >33 m/s) were common early in the record, but in the 1970s and 1980s wind speed decreased significantly. Of the total number of measurements (116 841), gale or stronger winds are observed 6.23% of the time, storm or above 0.34%, and hurricanes are observed 0.09% of the time. The high wind situations (>20 m/s) are associated with air temperatures between zero and –35 °C.

The general picture that emerges is that the relatively ice-free Kara Sea shelf is cooled by a negative radiation balance and cold air temperatures from September. During October  $T_a$  is about –10 °C and nearly all precipitation is snow. In November,  $T_a$  is ca. –20 °C and average wind speeds are close to 7 m/s. Storm episodes, which take place about 1.6 days every year on average, are likely to take place during the fall and winter.

For the model forcing, the full range—from

the mean (a moderate breeze) to a hurricane—is used (6, 12, 18, 24 and 30 m/s). The wind is directed along the coast in all runs. The highest wind episodes are of relatively short duration, so the storm (24 m/s) is applied over 24 h and the hurricane (30 m/s) over 12 h. In these cases, the model is started with 6 m/s during 6 h, then it is increased linearly to the given speed at 12 h. The wind speed is reduced over 6 h in the same way at the end.

The air temperature is set at a constant –10 °C. This is the mean between Dikson and Golomyanny meteorological stations in October. The snowfall is set at a constant 1 mm/day, which is close to the measured mean value of 26 mm/month shown in Table 2. The snow is divided equally over the five size classes for frazil ice. The model sensitivity towards  $T_a$  and snow is given in the section discussing sensitivity.

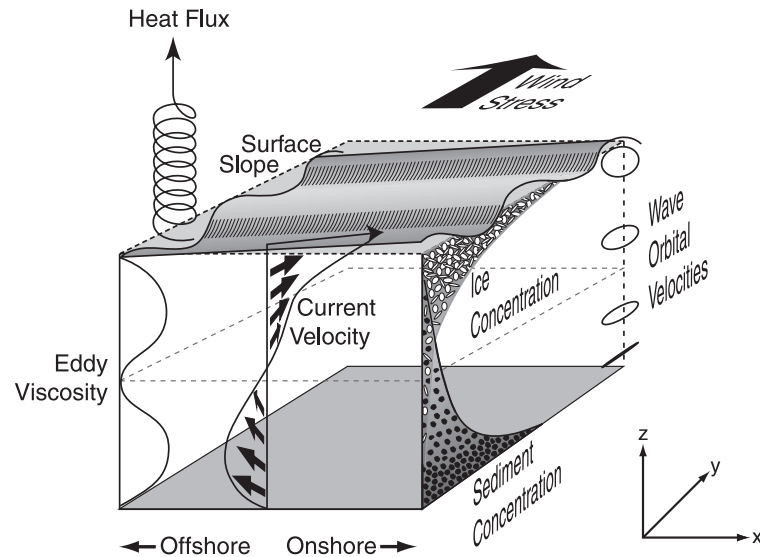
## The model

Frasemo is a vertical model that describes the state of a water column with time, as a result of surface forcing (wind, snow and  $T_a$ ). Horizontal current (along and onshore), salinity, temperature, (vertical) eddy viscosity and density are calculated in each vertical grid-cell. At the bottom, wave–current interaction resuspends sediment, and at the surface frazil ice crystals may form when the water is supercooled by a colder atmosphere. The different processes are illustrated in Fig. 6. Water density is calculated, including sediment and frazil ice concentrations. A more detailed description of the model is given by Sherwood (2000), where the model was

Table 2. Monthly mean atmospheric forcing on the Kara Shelf, August–December.

Parameter	Dikson Island					Golomyanny Island				
	Aug.	Sep.	Oct.	Nov.	Dec.	Aug.	Sep.	Oct.	Nov.	Dec.
$T_a$ (°C)	5.0	1.6	–7.3	–17.6	–22.3	0.0	–3.3	–12.0	–20.7	–24.2
Max $T_a$ (°C)	27	17	6	2	0	11	5	1	–1	0
Min $T_a$ (°C)	–12	–30	–43	–47	–49	–21	–36	–40	–46	–51
Rain (mm)	43	23	2			19	7			
Wet snow (mm)	3	16	8	1		6	10	3	1	1
Snow (mm)		6	24	19	20	3	6	15	11	11
Wind speed(m/s)	6.3	6.9	7.4	6.9	8.3	5.3	6.4	6.4	6.0	6.5
Max. speed (m/s)	34	28	>40	40	>40		30		29	31
Gale days (days)	4	5	8	8	10	2	4	5	4	5

Fig. 6. Schematic illustration of processes in the frazil and sediment model, Frasemo. The vertical model is initialized with temperature and salinity profiles, and is forced by winds, snow and air temperature. (Figure from Sherwood 2000; reproduced with permission of the American Geophysical Union and the author.)



developed and compared to analytic solutions for a variety of flows. The model runs presented here uses the Mellor–Yamada 2 1/2 turbulent closure model (Mellor & Yamada 1982).

Frasemo was developed further in Smedsrud (2002) to include size spectra for frazil crystals and sediment, secondary nucleation of frazil crystals and aggregation between sediment and frazil. The model was thus “upgraded” from the one-size assumption of frazil ice in Omstedt (1985) to a size spectrum approach (Svensson & Omstedt 1998), and verified against large tank laboratory experiments with 24 h duration (Smedsrud 2001). The frazil dynamics were shown to be adequately represented and the efficiency of the aggregation process was empirically estimated through an aggregation factor  $\alpha$ . The range of the five size classes for the frazil crystal diameter is 25  $\mu\text{m}$ –1.5 cm, and 1.15  $\mu\text{m}$ –625  $\mu\text{m}$  for the sediment grain diameter (Smedsrud 2002). The SPM is assumed to be in the smallest size group (diameter < 2  $\mu\text{m}$ , clay). The sediment grain size distribution at the bottom is set as a five class approximation of the measured sizes shown in Fig. 5. This yields 5.4% clay, 36.0% fine and medium silt, 37.5% coarse silt, 20.9% fine sand and only 0.2% medium and coarse sand.

A time step of 2.0 s and a vertical grid spacing of 0.2 m is used in the calculations. Due to the high velocities associated with the storms and hurricanes, the vertical grid spacing in these runs had to be increased to 0.4 m to prevent the bottom

roughness from being bigger than the grid spacing in the wave–current boundary layer.

The following values were discussed in Smedsrud (2002). (i) A size-dependent growth of frazil ice is modelled using a constant Nusselt number,  $N_u = 1.5$ . (ii) Secondary nucleation uses a maximum number concentration of crystals at each level ( $n_i$ ), equal to  $1.0 \times 10^3$ . (iii) The aggregation factor  $\alpha$  equals 0.005, the mean value. (iv) Size-dependent rise and sinking velocities are constant for each size. An upper limit for the sediment concentration aggregated to frazil ice crystals has not been found. As IRS concentrations in the laboratory experiments used to estimate  $\alpha$  were quite low—ca. 100 mg/l (Smedsrud 2001)—such an upper limit was not discussed when developing Frasemo.

Frazil ice crystals are modelled to start melting when the temperature is above the freezing point. The melting rate is given by the turbulent heat conduction where melting is taking place all over the crystal surface, not just the edge of the frazil disk.

The other standard parameters specified are the same as in Sherwood (2000) for turbulence, heat flux and sediment resuspension. The size dependent critical shear stress is calculated based on Gelfenbaum & Smith (1986), falling in the range 0.003–0.34  $\text{N/m}^2$ .

Tidal currents are observed to be quite strong (ca. 50 cm/s), but are not incorporated into the model. This is somewhat compensated for by

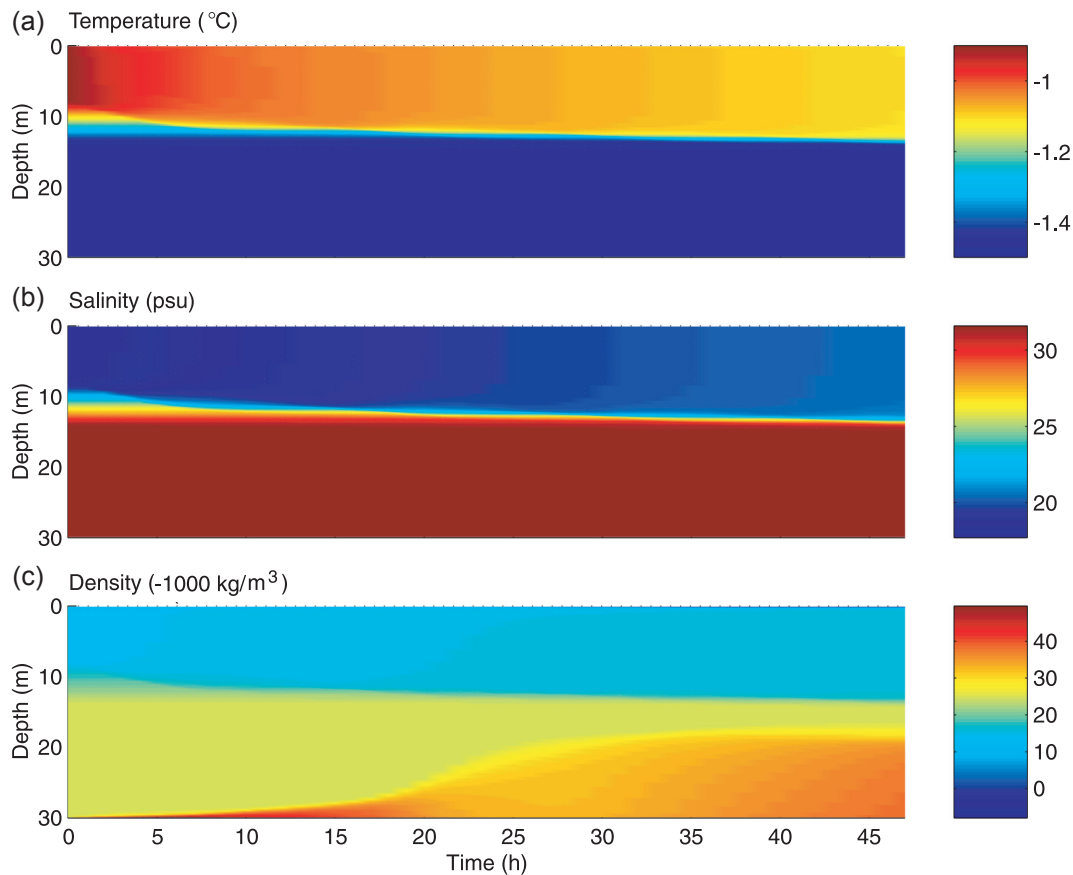


Fig. 7. Model results for the base case: (a) temperature; (b) salinity; and (c) density anomaly.

using in situ sediment concentrations from the shelf, reflecting the steady situation in the case of calm atmospheric conditions.

A vertical model has obvious limitations in calculating the mixing of an upper and lower layer in that it cannot account for horizontal advection. This mixing is also found to be quite sensitive to the initial salinity profile, the depth and the wind forcing. The depth and the stratification have opposite effects: the shallow water is usually more stratified than the deeper water.

## Model results

Results are first presented with respect to the 30 m depth and 18 m/s winds “base case”. Other cases with varying wind forcing over the same depth are presented subsequently, followed by the other depths (10 and 50 m) and the profiles

from the shelf. Results are given as mass concentrations of ice and sediment per litre of water for all parameters. This implies that the porosity of frazil ice and sediment are not accounted for and that bulk densities of the hybrid aggregates would be significantly smaller if the densities could be measured including the pore water. This is consistent with rise and sinking velocity calculations that use pure ice and sediment densities as given in Tables 1 and 2 in Smedsrud (2002).

### *Base case, 30 m depth outside the estuary (Area E)*

The model is started from rest and the gale (18 m/s) is set constant for the 48 h model run. The initial stratification is “E 30 m” presented in Table 1. The gale produces an upward heat flux of 220 W/m<sup>2</sup>. This makes ice start freezing after 2 h, when the surface has cooled slightly below the

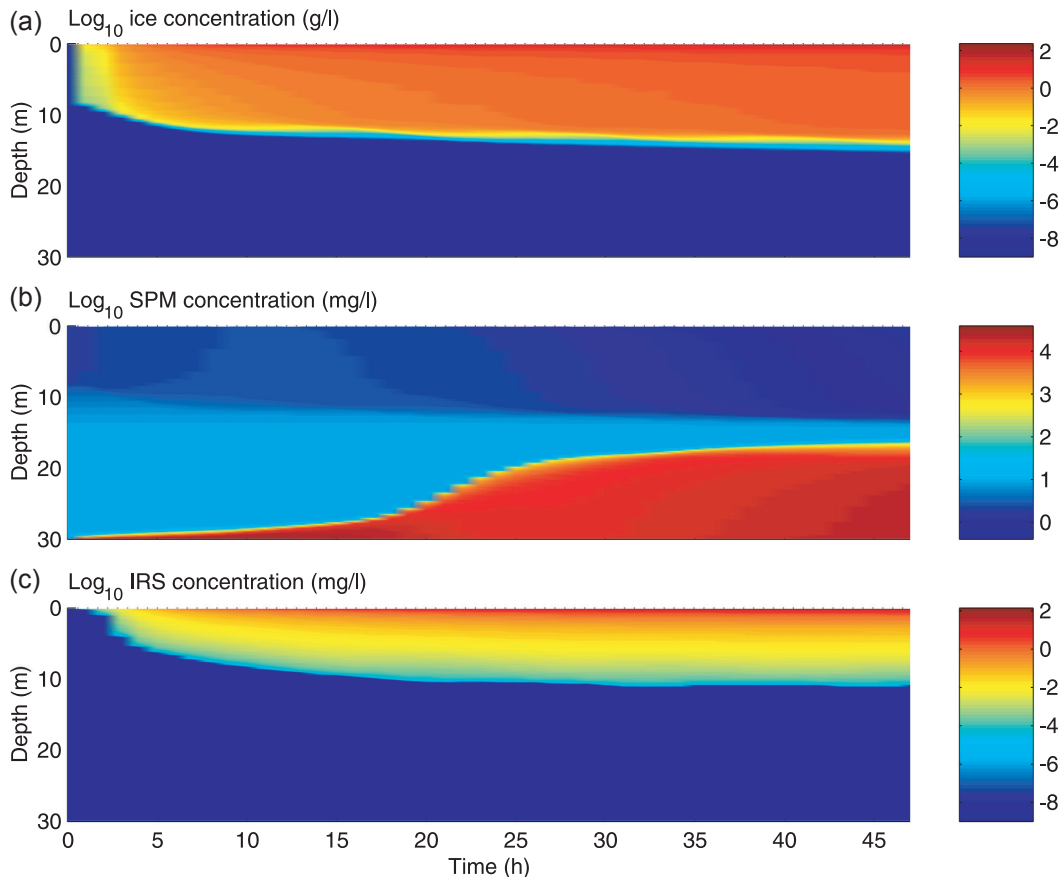


Fig. 8. Model results for the base case: (a) frazil ice concentration; (b) suspended particulate matter (SPM); and (c) ice-rafted sediments (IRS).

freezing point ( $T_f$ ) of  $-0.96^\circ\text{C}$ . Due to the presence of ice crystals from the snow, ice growth starts at once. Supercooling remains low, only ca.  $0.001^\circ\text{C}$ . The upward heat flux both cools and freezes the water, and after 48 h about  $80\text{ kg/m}^2$  of ice is produced. The evolution of temperature is plotted in Fig. 7a.

The upper layer salinity increases from 17.7 to 20.5 psu over the 48 h (Fig. 7b), due to both ice formation and mixing with the water in the 7 m thick halocline.

The 18 m/s wind blowing along the coast creates an Ekman transport with a speed of ca. 40 cm/s towards the coast (to the right in Fig. 6) in the upper layer, and an outwards compensating current in the lower layer, which balances the on/off shelf transport. Within 6 h the velocities are almost in a steady state and the offshore velocity in the lower layer is about 35 cm/s. At 6 h the alongshore velocities are close to 1 m/s at

the surface, decreasing to 20 cm/s at the bottom, increasing slowly with time.

The gale produces waves with a wave height of 3.4 m and a period of 7.0 s. The waves and the bottom stress from the current combine to resuspend sediment from the bottom. Consequently SPM increases steadily in the lower layer, making the lower layer denser (Fig. 7c).

Frazil ice remains in the upper layer throughout the 48 h (Fig. 8a). As the proportion of large crystals increases with time, more and more frazil gathers at the surface. Surface concentrations increase from 10 g/l at 10 h to 115 g/l at 30 h, and 234 g/l at the end.

At the end of 48 h, the total SPM is  $240\text{ kg/m}^2$ , but nearly all of it is in the lower layer with concentrations of about 20 g/l (Fig. 8b). In the upper layer, the initial 2 mg/l is decreased to less than 1 mg/l by the transformation to IRS through aggregation with frazil ice.

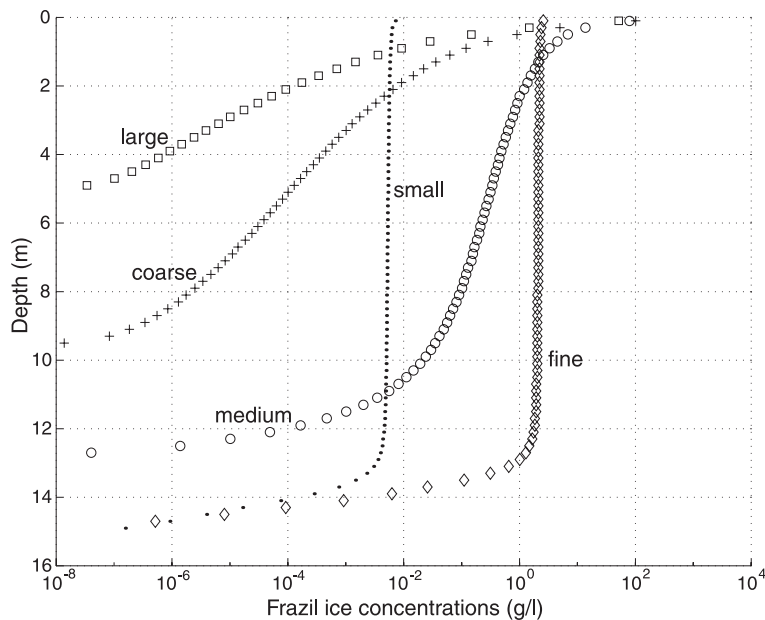


Fig. 9. Frazil ice concentration in the upper layer at 48 h (base case). The size classes are shown.

The IRS concentration in the surface increases steadily with time (Fig. 8c). Surface IRS reaches 35 mg/l in 24 h and 137.8 mg/l in 48 h, with 5.8 mg/l at 0.5 m depth. The IRS, like the SPM, consists of pure clay. In the lower layer where the SPM concentration reaches 20 g/l, 66.8% consists of clay, 31.6% of fine and medium silt and 1.6% of coarse silt.

Figure 9 shows the frazil ice concentrations plotted against depth at 48 h for the different size classes. The concentration of the smallest crystals is homogeneous down to 14 m depth and the larger crystals are more confined to the surface. The mass of frazil at 10 m depth increases from 0.5 g/l at 5 h to 2.0 g/l at the end. As seen in Fig. 9, this is in the range of the small to medium classes, with corresponding low rise velocities (Smedsrud 2002). The surface layer is about 0.2 m thick; the concentration at 0.3 m is 22.6 g/l and at 0.5 m 10.2 g/l. Surface size distribution is 0.0, 1.1, 33.8, 43.2 and 21.9% for the five classes, from the smallest to the largest.

After 10 h, more than 99% of the frazil ice is aggregated to sediment. The density of this ice is given by Eq. (17) in Smedsrud (2002). Due to the relatively low IRS concentration, this density is increased by less than 1 kg/m<sup>3</sup> from the pure ice density of 920 kg/m<sup>3</sup>. The frazil ice rise velocity is therefore decreased less than 1 mm/s for the largest crystals (and less for the smaller ones).

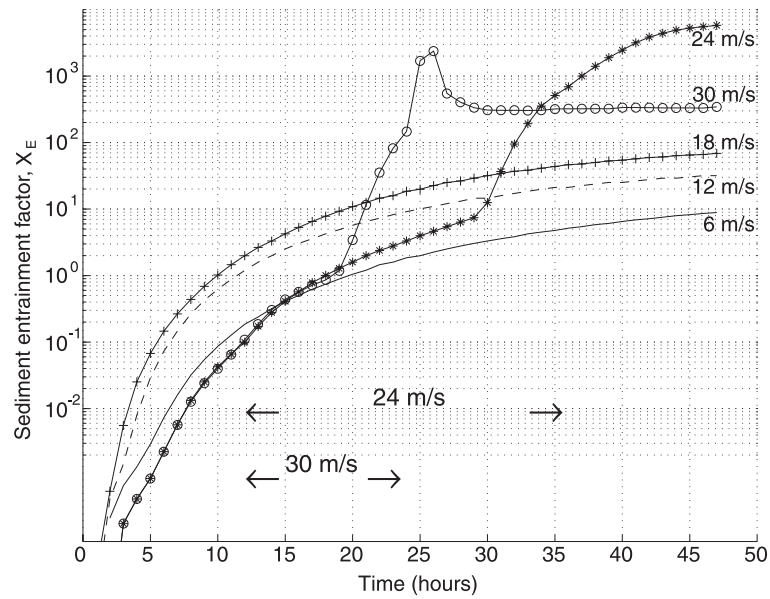
#### Area E: 30 m depth

The moderate breeze (6 m/s) produces an SPM concentration in the lower layer at 48 h of 1 g/l, compared to 20 g/l in the base case. In the upper layer SPM stays close to the initial value of 2 mg/l, producing an IRS of 17.8 mg/l at 48 h. The frazil ice stays in the upper 5 m, reaching 100 g/l at the end of the run.

With the strong breeze (12 m/s), the lower layer SPM increases to around 6 g/l at 48 h and the surface IRS reaches 63.6 mg/l. The surface ice concentration ends up at 194.3 g/l and there is about 1 g/l at 10 m depth.

The storm (24 m/s) lasts for 24 h, as indicated in Fig. 10, is imposed linearly over 6 h from a moderate breeze over the first 6 h and ceases in the same way at the end. The stratification is weakened, but the layers persist. The lower layer SPM is ca. 27 g/l at the end and in the upper layer ca. 500 mg/l. This produces a surface ice layer with 124 g/l of ice, an IRS of 11.6 g/l and a density of 975 kg/m<sup>3</sup>. There is a homogeneous ice concentration of 2 g/l down to 12 m depth, with less than 1 mg/l of sediment. A very small portion of the crystals makes it down into the lower layer. These crystals aggregate to sediment so efficiently that their buoyancy is lost, their density increases above that of the water and they sink to the bottom. At 48 h there is 1 g/l of this ice, with

Fig. 10. Entrainment factor: surface IRS concentrations divided by initial SPM, for the E 30 m depth cases with different wind forcing, as indicated.



a density  $1422 \text{ kg/m}^3$ .

The hurricane (30 m/s) lasts from 12-24 h, and ceases in the same way as the storm to the 6 m/s mean wind speed (Fig. 10). At 48 h the upper layer salinity has increased to 24.8 psu. The lower layer has decreased to 27.7 psu. Sediment is resuspended during the 12 h and does not deposit with the 6 m/s wind. The SPM in the lower layer is about 20 g/l from 24 to 48 h. In the upper layer SPM increases from ca. 300 mg/l at 24 h to 1 g/l at 48 h. Due to the very strong turbulence, the ice is diffused efficiently downwards at 24 h, ice concentrations decreasing gradually with depth from 4.3 g/l at the surface to 0.5 g/l at 15 m depth. The ice is buoyant down to 25 m depth at this stage and the surface IRS is 160 mg/l. At 48 h the ice in the upper layer is well mixed, with around 4 g/l down to 10 m depth. The surface IRS has reached 691.6 mg/l and the IRS concentration is around 400 mg/l in the upper 10 m. The ice has negative buoyancy below and IRS concentrations reach 2 g/l.

An entrainment factor,  $X_E = (\text{IRS}/\text{SPM})$ , is plotted for the five different wind speeds over the Area E 30 m water column (Fig. 10). The initial SPM value of the upper layer of 2 mg/l is used. Figure 10 shows that it takes between 10 and 20 h for the surface ice to reach the initial SPM concentration of 2 mg/l. As the hurricane changes to a moderate breeze over the course of 24 to 30 h, there is only a very slight increase in the IRS after

30 h in this case.

#### Area E: 10 m depth

With a moderate breeze, sediment and frazil ice stay close to the bottom and surface, respectively. SPM in the lower layer is ca. 6 g/l at 48 h and the IRS reaches 21.7 mg/l. Surface ice concentration reaches 118 g/l.

With the strong breeze (12 m/s), the two layers also stay intact. The SPM concentration in the lower layer at 48 h is about 70 g/l—this is over three times as much as in the base case. This leads again to high surface SPM (ca. 400 mg/l) and IRS (10.5 g/l). There is about 4 g/l of frazil ice down to 5 m depth. At the bottom there is a small volume of sinking ice (1.6 g/l), loaded with 4 g/l of sediment.

The gale mixes the two layers in 16 h. Just before the mixing the SPM in the upper layer is ca. 700 mg/l and the surface IRS is 19.1 g/l. No sinking ice is formed, but this changes quickly. Just after the mixing the density of the hybrid aggregates increases to above  $1200 \text{ kg/m}^3$ . The rise velocity of the largest frazil crystals has changed from 28 mm/s in the pure state to a sinking velocity of 8 mm/s because of the aggregated sediment. At 48 h the sediment distribution is homogeneous, SPM is ca. 32 g/l and IRS is ca. 58 g/l, but there is more ice at the bottom (ca. 20 g/l) than at the surface. Density of the sinking

ice is close to 2000 kg/m<sup>3</sup>.

The storm is imposed gradually from 6 to 12 h and at 17 h mixing occurs. Before this there is a thick layer of ice in the surface, increasing from 2 g/l at 5 m depth to 10 g/l at the surface. The surface ice has an IRS of 440 mg/l and a density of 945 kg/m<sup>3</sup>. Soon after this the ice starts to sink.

The hurricane mixes the two layers fully at 15 h; before this the surface layer of ice (5 g/l) has an IRS of 185 mg/l. The ice starts to sink shortly after homogeneous concentrations are reached. The ice concentration is “turned around” from the normal state, with no surface ice and about 14 g/l at the bottom, loaded with 57 g/l of sediment.

#### Area E: 50 m depth

At this depth the moderate breeze resuspends little sediment and the only SPM in the upper layer is the initial value of 2 mg/l. As frazil ice is confined to the upper layer, the IRS reaches only 2.9 mg/l, with an ice concentration of 31.6 g/l.

The strong breeze is able to diffuse some frazil ice (ca. 1 g/l) down to 10 m depth, but the SPM is as low as with the moderate breeze. This increases the surface IRS at 48 h to 17.0 mg/l. The average upward heat flux is increased from 73 to 144 W/m<sup>2</sup> with the stronger wind. The surface ice concentration becomes 65 g/l at the end of the run.

The gale resuspends sediment, but only to 15 m above the bottom. The heat flux is given by the forcing: 220 W/m<sup>2</sup>, which is equal to the base case. Frazil ice is diffused further down into the surface layer, about 2 g/l at 15 m depth at the end. The surface IRS becomes 37.1 mg/l in 87.8 g/l of ice.

The storm resuspends sediment in the lower

layer and diffuses frazil ice down to the halocline at 20 m depth. At the end of the turn the surface has 106.6 g/l of ice, with an IRS concentration of 53.0 mg/l.

The hurricane manages to resuspend enough sediment so that the upper layer SPM is increased to 3 mg/l. Frazil ice is diffused down to the halocline with 1 g/l from 4-15 m depth. At 2 m depth there is 3 g/l of frazil ice, and in the surface 78.5 g/l, with an IRS concentration of 24.6 mg/l. This seems to be less than in the case with the storm, but the IRS is just vertically more distributed (Table 3). Integrated over the surface ice layer, this is the largest IRS concentration for the 50 m depth cases, as expected.

#### Shelf profiles

The three stratifications chosen as typical for the shelf area between the Ob and Yenisey estuaries and Severnaya Zemlya are given in Table 2. As the forcing is the same as for Area E, this also forms a sensitivity study for the stratification, and to some degree also for the initial SPM concentration, which both are lower in this area. Changes from the E cases are described below.

In the 10 m case with moderate breeze the upper layer SPM remains lower than in Area E, resulting in a lower surface IRS concentration: 6.9 mg/l. With the strong breeze, the sediment from the lower layer diffuses more easily than in Area E and the upper layer SPM increases to about 500 mg/l, increasing the IRS at the end to 15.0 g/l. The gale needs 1 h less to mix the two layers compared to the Area E case and the sinking ice density is further increased to 2200 kg/m<sup>3</sup>. The storm and the hurricane mix the less stratified layers more easily and the ice becomes even more loaded with sediment.

Table 3. Calculated IRS concentrations (g/m<sup>2</sup>) after 48 hours in turbid sea ice for different water columns and wind speeds on the Kara Shelf. Area is given in percent of the total area of 216850 km<sup>2</sup> for each column. Cases where all the ice becomes negatively bouyant and tends to sink are indicated with –. Total is given in tonnes.

	E 10 m	E 30m	E 50 m	S 10 m	S 30 m	S 50 m	Total
Area	21.5	15.2	5.5	32.9	16.0	8.9	100
6 m/s	4.3	3.6	0.6	1.4	1.1	0.3	0.5 × 10 <sup>6</sup>
12 m/s	2104.6	12.7	3.4	3006.6	4.7	1.5	313.3 × 10 <sup>6</sup>
18 m/s	–	33.2	7.4	–	19.1	3.2	1.9 × 10 <sup>6</sup>
24 m/s	–	4715.8	10.6	–	9460.7	4.6	483.9 × 10 <sup>6</sup>
30 m/s	–	4435.9	12.4	–	7487.2	79.0	407.7 × 10 <sup>6</sup>

For 30 m depth, the moderate and strong breezes lead to smaller surface concentrations of IRS than in Area E because of the lower initial SPM. With the gale, the weaker stratification leads to an increase in the SPM in the upper layer at about 46 h. Because this happens so late in the integration, the surface IRS concentration becomes lower than in the base case, again because of the lower initial SPM. The storm resuspends more sediment with the weaker stratification, resulting in an upper layer with a close to homogeneous concentration of 5 g/l of frazil ice with an IRS of ca. 500 mg/l and a density of ca. 980 kg/m<sup>3</sup>. The hurricane is close to mixing the upper layer with the lower, but at 48 h there is still a halocline of 1 psu. The flux of SPM into the upper layer is efficient. The SPM ends at 2.4 g/l. The ice in the surface layer is very close to neutrally buoyant, ca. 1025 kg/m<sup>3</sup>, but below 10 m depth the ice sinks. The surface ice layer is 10 m thick, has ca. 5 g/l of ice and about 800 mg/l of sediment.

In the 50 m cases, the moderate and strong breezes and the gale give low IRS concentrations due to the low initial SPM. The storm is able to increase the upper layer SPM slightly and during the hurricane the SPM flux to the upper layer is larger than in Area E because of the weaker stratification.

### Overview

Model results for vertically integrated IRS concentrations at 48 h are given in Table 3. Only IRS that is aggregated to ice and has a density lower than the upper layer is included in the integration. The stratifications used (Area E 10 m to Area S 50 m) are given in Table 2. For each wind speed the IRS concentration for each water column is multiplied with the respective area to form the total values. The unit, g/m<sup>2</sup>, is equivalent to tonnes/km<sup>2</sup>.

The lowest wind speed, the moderate breeze, is also the mean wind speed in the area. This wind produces the smallest IRS mass as expected. The IRS mass is increased by three orders of magnitude with a freeze-up during a strong breeze.

Table 3 shows the surprising result that the total mass of IRS does not increase monotonically with wind speed. The formation of frazil ice with negative buoyancy due to the aggregated sediment makes the IRS mass for the gale case lower than that for the strong breeze. As the ice in half the area (Area E 10 m + Area S 10 m) sinks,

this effect becomes very important. The storm produces the largest mass of IRS, the hurricane slightly less. This is because the increased IRS concentration in Area E 50 m and Area S 50 m, due to the stronger wind, is lost in sinking IRS in the Area E 30 m and Area S 30 m areas.

At low wind speeds a higher IRS mass is reached with the higher initial SPM concentrations in the upper layer of Area E. At higher wind speeds Area S produces more IRS because of the weaker stratification. The transition takes place with a moderate breeze for 10 m, a storm for 30 m and a hurricane for 50 m depth.

### Discussion

The transition from free-floating frazil ice crystals to slush ice is a gradual process. The upper layer of crystals gradually becomes more compact. At some stage congealing starts between crystals, forming turbid sea ice: granular ice with IRS. The transition is not well defined. Sherwood (2000) stated that all model assumptions valid for water are also valid for the ice–water mixture until the surge ice concentration has reached 10 g/l, or 1%. In their experiments with wave damping by grease ice, Martin & Kauffman (1981) suggest that the transition from the free-floating frazil ice stage to the wave damping stage occurs at a concentration of 200 g/l.

The transfer of momentum between the air and water is the source for turbulence in the calculations. The transfer of turbulent kinetic energy from the surface and down into the water is dependent upon the surface roughness length ( $z_0$ ), which should change when the surface ice layer changes. Alam & Curry (1998) suggests that  $z_0$  changes significantly when the ice concentration reaches 400 g/l, when the grease ice starts to behave like a solid. The transition for the surface heat flux is parameterized in the same way as for momentum and again an ice concentration of 400 g/l is given as the critical value (Alam & Curry 1998).

The thickness of the frazil ice layer can be estimated using the parameterization of Alam & Curry (1998). The frazil ice layer thickness is not defined explicitly because the horizontal approximation does not allow for a frazil ice depth profile. Using as a definition for the bottom of the frazil layer in Frasemo the depth at which 90% of the ice mass is reached in a vertical integral,

starting at the surface and working downwards, gives a frazil layer thickness of 0.5 m (Fig. 9). This is comparable to the frazil pile-up depth in Alam & Curry (1998), using a fetch of 1000 m and the 18 m/s gale of the base case. The slush ice will keep the thickness until it is transformed into solid ice.

The surface layer of frazil is about the same thickness as the vertical grid spacing (20-40 cm), supporting the idea that the model results describe the physical processes until the frazil ice concentration is on the order of 200 g/l. The upper cell is representative of the surface ice layer and flux parameterizations at the surface are valid until an ice concentration of 400 g/l is reached. As the maximum ice concentration described here is 234 g/l (base case), this implies that the 48 h model runs presented here can all be regarded as “open water”. Thus the entire Kara Sea will be exposed to the described processes during the first 48 hours of the autumn freeze-up every year.

The surface heat flux will decrease sometime after the first 48 hours as a result of the thicker and more solid ice cover that insulates the underlying water due to its low heat conductivity. A 0.2 m thick solid ice cover with  $T_a = -10^\circ\text{C}$  produces a heat flux of about 3 W/m<sup>2</sup> (Ono 1968), in contrast with the 220 W/m<sup>2</sup> in the base case.

### Sensitivity

Frasemo is tested for different forcing, a shorter fetch, for variation in the empirical aggregation factor and for flocculation. The stratification from the base case, Area E 30 m, is used. Because the storm case is such an important contributor to the

total IRS mass, the analyses are performed with this wind speed. Values are tabulated in Table 4 for each case.

An air temperature of  $-20^\circ\text{C}$  increases the average upward heat flux from 220 W/m<sup>2</sup> in the base case to 470 W/m<sup>2</sup>. This creates a more concentrated ice layer at the surface and down to 12 m depth. There is an increase in the IRS concentration because of the higher ice concentrations. Raising  $T_a$  to  $-5^\circ\text{C}$  leads to an upward heat flux of 96 W/m<sup>2</sup>. At the the surface, and in the upper layer, ice concentration decreases.

Increasing the precipitation (snow) leads to an increased surface ice concentration and a corresponding IRS increase. Decreasing the precipitation decreases the surface IRS concentration as well. The frazil ice size distribution is changed significantly to larger crystals, which again leads to less frazil ice in the upper layer and more at the surface.

The size class averaged value of the aggregation factor estimated in Smedsrud (2002) was  $\alpha = 0.005$ . This has been used in all cases up to now. The observed range of IRS in the laboratory experiments gave the range 0.0003-0.1 for the empirically determined constant. Using  $\alpha = 0.05$  makes some of the ice sink; there is 13 g/l of ice at the bottom with a density of 1900 kg/m<sup>3</sup>. In the upper layer the ice is neutrally buoyant. At the lower end of the range,  $\alpha = 0.0005$  makes all the ice buoyant, with a density close to 920 kg/m<sup>3</sup>. The ice has a small sediment load at all depths.

To include the effect of flocculation in a simple way, the smallest sediment size in the model (clay) is increased to 11.0  $\mu\text{m}$  (same as the fine and medium silt). The sinking velocity is set as half way between the two classes. This does not

Table 4. Sensitivity of Frasemo to different forcing and parameters with storm winds (24 m/s). Values are given at 48 hours for the surface layer. The initial stratification is from 30 m depth in Area E (E 30 m).

Name	Change	Ci max (g/l)	IRS (g/l)	$\Sigma$ IRS (kg/m <sup>2</sup> )
E 30 m, 24 m/s wind		125	11.6	4.7
Cold	$T_a = -20^\circ\text{C}$	331	19.6	7.9
Warm	$T_a = -5^\circ\text{C}$	30	2.8	1.1
More snow	10 mm/day	149	13.7	5.5
Less snow	0.1 mm/day	151	11.3	4.5
High aggregation	$\alpha = 0.05$	5	0.9	12.8
Low aggregation	$\alpha = 0.0005$	126	2.7	1.1
Flocculation	clay = silt	138	14.5	5.8
Short fetch	fetch = 5 km	60	9.1	3.7

change the SPM concentrations, but the size of the initial SPM is larger, making the probability for collisions higher.

A smaller fetch can be used to simulate the conditions in a winter polynya to some degree. A fetch of 5 km decreases the wave height to 0.95 m, compared to 3.4 m with the 100 km fetch in the base case. This decreases the sediment resuspension from the bottom.

#### *Cooling of the lower layer through melting of frazil ice*

If the frazil ice crystals formed in the upper layer are mixed down into water slightly above the freezing point, they will start to melt. They will then melt at the in situ freezing point, and thus be able to make the water supercooled compared to the surface. This is discussed more thoroughly in Smedsrud (2000). All frazil ice crystals are modelled to melt and a specific volume, representing a specific number of crystals, are transferred from a larger to a smaller size group.

The model shows that it takes quite strong forcing to cool the lower layer on the Kara Shelf to the surface freezing point. As the upper layer reaches its freezing point, it is likely that cooling of the lower layer takes place through formation of frazil ice, as well as through inclusion of brine released during ice growth at the surface. Cooling of the lower layer to its in situ freezing point can only be done by frazil ice diffusing into the lower layer.

It is not clear what would happen if hybrid ice starts to melt. The process of disaggregation due to melting has not been addressed in this study.

#### *Ice-rafted sediment*

The difference in the IRS mass between the different model runs is caused by a combined effect of the SPM content of the water, the volume of ice at each level and the strength of the turbulence that causes the particles to collide and aggregate. The theoretical framework was described in Smedsrud (2002) and tested when the model was applied to available experimental data from a 1 m deep indoor tank. Contrasts between the modelled natural setting—the Kara Sea—and the experimental data are highlighted below.

The aggregation factor ( $\alpha$ ) is an empirical value, verified on measured levels of IRS up to ca. 100 mg/l (Smedsrud 2001). In the present

model runs, IRS concentrations reach values two orders of magnitude larger than this value, at which stage the ice aggregated to sediment starts to sink. As the experimental data do not cover the high IRS cases, these values should be treated with caution; they may overestimate the IRS concentrations.

Observations of frazil ice with high sediment loads at the bottom are reported from the Beaufort Sea (Reimnitz et al. 1987). Such ice was also tentatively identified in at one location (floe 4) in the Kara Shelf sea ice (Smedsrud & Eicken 2003), where the maximum IRS concentration was 536 mg/l. Such ice is called “anchor ice” if the frazil aggregates to particles at the bottom, but as the frazil ice modelled here aggregates to SPM in suspension the term “sinking ice” has been used. The concentration of IRS in the sampled anchor ice is higher than the theoretical value from the available area on a frazil ice disk. Therefore, an upper limit of the IRS concentration has not been implemented in the model. If such a limit had been introduced, sinking ice would not have been formed.

The sediment used in the experiments did not come from the Kara Shelf, but the size distribution of the sediment in the experiment and on the Kara Shelf is similar. It is uncertain to what degree  $\alpha$  could change between different types of sediment. Heat fluxes of the model and the experiment do not differ significantly, supporting the assumption that the same processes govern the frazil ice growth.

The base case rms velocity was 5-10 cm/s, directly comparable to the experimental conditions. For the four experiments in Smedsrud (2001) the rms velocity was in the range of 4-12 cm/s, but was mostly between 6 and 10 cm/s. In contrast, the turbulent dissipation rate in the model runs was about  $50 \times 10^{-6}$  W/kg, roughly ten times higher than the value of the 10 cm/s current experiment (mean  $\epsilon = 3.7 \times 10^{-6}$  W/kg) and ten times lower than that of the other experiments (mean  $\epsilon = 380 \times 10^{-6}$  W/kg) with a current of 30 cm/s.

The vertical eddy viscosity ( $K_z$ ) in the upper layer of the base case is about  $10.0 \times 10^{-3}$  m<sup>2</sup>/s. As  $K_z$  is calculated based on  $q$  and  $\epsilon$ , both in the simple case of the experiments and in the Mellor–Yamada turbulent closure in Frasemo, this value reflects the differences in  $\epsilon$ . The 10 cm/s current experiment had a  $K_z$  ten times larger than in the base case (ca.  $110.0 \times 10^{-3}$  m<sup>2</sup>/s), but in the other

three 30 cm/s current experiments it is roughly the same:  $K_z$  equals ca.  $3.7 \times 10^{-3} \text{ m}^2/\text{s}$  (Smedsrud 2001). The results given in Table 3 for the IRS content of the first Kara Shelf surface ice cover of the season should therefore be quite representative within the limitations of a vertical model approach.

Clay is known to flocculate when it enters the ocean. This may lead to significantly larger particles, in the range of 10–20  $\mu\text{m}$ , which have a higher sinking velocity than a single clay particle. The sinking velocity is not as large as for the silt grains of the same size, as the flocculated particles contain a significant portion of water. If the initial SPM of the upper layer were flocculated, this would lead to a faster transformation to IRS, as demonstrated in the sensitivity section. Resuspension of flocculated sediment from the bottom would probably need higher critical shear stresses. Because of the greater sinking velocities, upward turbulent diffusion of flocculated clay is less efficient than for pure clay and this may lead to lower SPM in the low wind cases. As high concentrations of resuspended sediment in the upper layer leads to sinking frazil ice in the cases with strong winds, moderately lower SPM concentrations might actually lead to a higher buoyant IRS mass in these cases.

During the first freeze-up of the season frazil ice is probably diffused down into the warmer lower layer, given a strong enough wind. Here the crystals start to melt, but in these cases a large portion of the ice also becomes negatively buoyant and starts to sink. This process is not addressed in this study and it is uncertain if this combination of sinking and melting would lead to a lower or higher IRS content of the surface ice. The frazil ice that sinks might actually lose most of its aggregated sediment, thereby gain buoyancy, floating up to the surface while still carrying a significant IRS mass. In the cases where the upper mixed layer stays intact, frazil ice also largely stays there and little significant melting occurs, even with a warmer layer underneath.

During autumn, there might actually be more than one freeze-up. The first ice cover may be advected by the winds northwards towards the Arctic Ocean or the thin ice may be efficiently rafted/ridged against the coast to form fast ice, thus leaving an open area further off coast. The water columns will probably become less stratified, regaining their stratification due to the inflow of river water and denser water from the

Arctic ocean as a part of the compensating estuarine circulation. The water will now be at, or at least closer to  $T_f$  than the data from September suggest and as assumed during the described cases.

The modelled IRS concentrations are comparable to IRS measured in turbid ice on the Kara Shelf (Smedsrud & Eicken 2003). The IRS concentrations from the moderate breeze are similar to the lowest values below 10 mg/l. The maximum IRS concentration found in the sea ice was 2.6 g/l, and this is at the same level as the maximum IRS concentrations found in this study: 10–15 g/l in the 10 m cases with the moderate breeze. In a study where the trajectories of sediment laden ice were tracked backwards from their sampling location in the central Arctic Ocean to the Kara Sea the range was 10 mg/l–10 g/l (Pfirman et al. 1997).

The total values of the IRS mass in Table 3 are significant compared to the annual river supply of  $29 \times 10^6$  tonnes. The lowest value from the mean climatological winds, a moderate breeze, is  $0.46 \times 10^6$  tonnes, or 1.6% of the total discharge. So if the major portion of the ice cover freezes during a calm period, much of the sediment stays at the bottom.

The situation changes drastically with a freeze-up during a strong breeze, when the IRS mass is comparable to 10 years of sediment discharge by rivers. This high value may indicate that major portions of the IRS do not leave the Kara Sea. The IRS fraction from the 10 m areas are very large and may indicate that this ice becomes a part of the fast ice cover, which stays in place during the winter and melts on the shelf during the spring and summer period. Another explanation of the high values could be that there are significantly coarser sediment in the 0–20 m depth areas and that the grain size distribution used (Fig. 5) is not very representative here. This would lead to artificially high levels of SPM and, consequently, IRS as well. However, the high numbers also indicate that the export of IRS holds a potential for being the major pathway out of the Kara Sea for the sediment discharged by the rivers.

With the gale winds of the base case forcing, the total IRS mass is 6.5% of the total river discharge, there is no contribution from the 0–10 m areas and the grain size distribution should be more representative for the contributing area.

For the storm and hurricane cases, the total IRS mass is comparable to 10–15 years of sedi-

ment discharge. While these are high values, it is unlikely that the freeze-up takes place during such an episode as these winds are observed only 0.43% of the time at Dikson. In these cases there are no contributions from the fast ice area, but the high values of the 30 m cases are associated with high levels of SPM due to the efficient resuspension by the waves and currents. Such resuspension may be reduced if the layer below the loose surface sediment layer were compact.

Confidence in the IRS mass estimates presented in this work could be significantly increased if more measurements of the Kara Shelf sediment were available. This is true for both volumes of SPM (during different wind forcing) and grain size of bottom sediment in specific areas.

## Conclusion

Formation of turbid sea ice—granular ice with incorporated ice-rafted sediment (IRS)—may be efficient on the Kara Sea shelf during the autumn freeze-up. In shallow areas (<20 m depth), the process can be effective with low winds (ca. 12 m/s). In the deeper areas (>20 m depth), the strong salinity stratification implies that for an effective production of IRS winds above 18 m/s or a reduced stratification of the water column are needed. For the rest of the winter months there may be additional IRS incorporated in ice formation in a coastal polynya.

The large (200 000 km<sup>2</sup>) area is divided into three different depth zones (0–20 m, 20–40 m and 40–60 m), with two kinds of stratification. The areas close to the Ob and Yenisey rivers have a stronger stratification than the areas further north. The vertical model represents each area and during 48 h a surface slush ice cover is formed with ice concentrations typically in the range 100–200 g/l. In the mixed upper layer modelled ice concentrations are usually between 1 and 5 g/l.

A freeze-up with the climatologically mean wind speed of 6 m/s incorporates 2% of the annual sediment discharge by the Ob and Yenisey rivers into the ice. With higher winds some of the frazil ice crystals are aggregated to so much sediment that they gain negative buoyancy (a density > 1030 kg/m<sup>3</sup>) and sink.

With moderate breeze during freeze-up, very high values of IRS are produced in the 0–20 m area, comparable to 10 years of sediment dis-

charge. This sediment probably becomes a part of the fast ice along the coast and some, or most, of it is returned to the water when the fast ice melts on the shelf during summer. As there are very little data on surface sediments from this area, the assumption of similar size here as in the deeper areas might lead to an IRS mass that is too high. However, any new sediment deposited in this area over the summer will have a high probability of entering the ice as IRS.

For a freeze-up during a gale, about 6.5% of the yearly sediment discharge transforms to IRS. In this case results show that the ice in the shallow areas sinks due to the sediment load and the IRS contribution is only from the 20–60 m depths.

For a freeze-up with a storm or a hurricane, the IRS mass compares to 15 years of river sediment discharge. However, the chances for such winds during the freeze-up are small. On average there are 1.6 days with such winds every year. As the strongest winds blow during the winter period, the statistical chance for a freeze-up during such an episode should be about once every 50 years.

*Acknowledgements.*—The Dikson wind data are from the Carbon Dioxide Information Analysis Centre (<http://cdiac.esd.ornl.gov/ftp/ndp048>), prepared by V. N. Razuvaev, E. B. Apasova and R. A. Martuganov of the All-Russian Research Institute of Hydro Meteorological Information–World Data Centre. The Kara Sea surface salinity figures are from the University of Washington (<http://psc.apl.washington.edu/ANWAP>) and were originally produced at the Arctic and Antarctic Research Institute in St. Petersburg. The manuscript has benefited from comments by Carl F. Forsberg, Norwegian Polar Institute. This work was supported by Transport and Fate of Contaminants in the Northern Seas, a project coordinated by the Norwegian Polar Institute, and the Research Council of Norway (contract no. 71928/410).

## References

- Alam, A. & Curry, J. A. 1998: Evolution of new ice and turbulent fluxes over freezing winter leads. *J. Geophys. Res.* 103 (C8), 15 783–15 802.
- Alexandrov, E. I., Radionov, V. F. & Svyaschennikov, P. N. 2000: Chapter III. Climatic regime and its changes in the region of the Barents and Kara seas. In *Transport and fate of contaminants in the northern seas. Sea ice project package. AARI final report*. St. Petersburg: Arctic and Antarctic Research Institute. Available on the internet at <http://npolar.no/transeff/Transport/Ice/>.
- Carroll, J., Boisson, F., Teyssie, J.-L., King, S. E., Krosshavn,

- M., Carroll, M. L., Fowler, S. W., Povinec, P. P. & Baxter, M. S. 1999: Distribution coefficients for use in risk assessment models of the Kara Sea. *Appl. Radiat. Isot.* 51, 121–129.
- Carroll, J. & Harms, I. H. 1999: Uncertainty analysis of partition coefficients in a radionuclide transport model. *Water Res.* 33, 2617–2626.
- Dmitrenko, I., Golovin, P., Gribanov, V., Kassens, H. & Holeman, J. 1998: Influence of the summer river runoff on ice formation in the Kara and Laptev seas. In H. T. Shen (ed.): *Ice in surface waters*. Rotterdam: A. A. Balkema.
- Evenset, A., Dahle, S., Loring, D., Skei, J., Sørensen, K., Cochrane, S., Carroll, J. & Forsberg, C. F. 1999: *KAREX 94: an environmental survey of the Kara Sea and the estuaries of Ob and Yenisey*. Akvaplan-niva Rep. 414.96.1006. Tromsø: Akvaplan-niva.
- Gelfenbaum, G. & Smith, J. D. 1986: Experimental evaluation of a generalized suspended-sediment transport theory. In R. J. Knight & J. R. McClean (eds.): *Shelf sands and sandstones. Memoir 11*. Pp. 133–144. Calgary: Canadian Society of Petroleum Geologists.
- Gloersen, P., Campbell, W. J., Cavalieri, D. J., Comiso, J. C., Parkinson, C. L. & Zwally, H. J. 1992: *Arctic and Antarctic sea ice, 1978–1987*. Washington, D.C.: National Aeronautics and Space Administration.
- Hanzlick, D. & Aagaard, K. 1980: Freshwater and Atlantic water in the Kara Sea. *J. Geophys. Res.* 85(C9), 4937–4942.
- Harms, I. H. & Karcher, M. J. 1999: Modelling the seasonal variability of hydrography and circulation in the Kara Sea. *J. Geophys. Res.* 104(C6), 13431–13448.
- Johnson, D., McClimans, T., King, S. & Grenness, Ø. 1997: Fresh water masses in the Kara Sea during summer. *J. Mar. Syst.* 12, 127–145.
- Kempema, E. W., Reimnitz, E. & Barnes, P. W. 1989: Sea ice sediment entrainment and rafting in the Arctic. *J. Sediment Petrol.* 59, 308–317.
- Kowalik, Z. & Proshutinsky, A. Y. 1994: The Arctic Ocean tides. In O. M. Johannessen et al. (eds.): *The polar oceans and their role in shaping the global environment*. Washington D.C.: American Geophysical Union.
- Krosshavn, M., Carroll, J., Grennes, Ø., Johnson, D., King, S., Johnsen, A., Bjørnstad, H. & Engøy, T. 1997: *Environmental pollution and oceanography in the Arctic—EPOCA95. Tech. Rep. FFI/RAPPORT-97/02129*. Oslo: Norwegian Defense Research Establishment.
- Martin, S. & Kauffman, P. 1981: A field and laboratory study of wave damping by grease ice. *J. Glaciol.* 27, 283–313.
- Mellor, G. L. & Yamada, T. 1982: Development of a turbulent closure model for geophysical fluid problems. *Rev. Geophys. Space Phys.* 20, 851–875.
- Milliman, J. D. & Meade, R. H. 1983: World-wide delivery of river sediments to the oceans. *J. Geol.* 91, 1–21.
- Nürnberg, D., Wollenburg, I., Dethleff, D., Eicken, H., Kassens, H., Letzig, T., Reimnitz, E. & Thiede, J. 1994: Sediments in Arctic sea ice: implications for entrainment, transport and release. *Mar. Geol.* 119, 184–214.
- Nygaard, E. 1995: *Cid-report from KAREX 94*. Nor. Polarinst. Rapp.ser. 90. Oslo: Norwegian Polar Institute.
- Omstedt, A. 1985: Modelling frazil ice and grease ice formation in the upper layers of the ocean. *Cold Reg. Sci. Technol.* 11, 87–98.
- Ono, N. 1968: Thermal properties of sea ice. *Low Temp. Sci.* A23, 329–349.
- Osterkamp, T. E. & Gosink, J. P. 1984: Observations and analyses of sediment-laden sea ice. In P. Barnes et al. (eds.): *The Alaskan Beaufort Sea: ecosystems and environments*. Pp. 73–93. Orlando: Academic Press.
- Pavlov, V. K. & Pfirman, S. L. 1995: Hydrographic structure and variability of the Kara Sea: implication for pollutant distribution. *Deep Sea Res.* II 42, 1369–1390.
- Pfirman, S., Colony, R., Nürnberg, D., Eicken, H. & Rigor, I. 1997: Reconstructing the origin and trajectory of drifting Arctic sea ice. *J. Geophys. Res.* 102(C6), 12575–12586.
- Reading, H. G. 1996: *Sedimentary environments: processes, facies and stratigraphy*. Oxford: Blackwell Science.
- Reimnitz, E., Kempema, E. W. & Barnes, P. W. 1987: Anchor ice, seabed freezing, and sediment dynamics in shallow Arctic seas. *J. Geophys. Res.* 92(C13), 14671–14678.
- Sherwood, C. R. 2000: Numerical model of frazil-ice and suspended-sediment concentrations, and formation of sediment-laden ice in the Kara Sea. *J. Geophys. Res.* 105(C6), 14061–14080.
- Smedsrud, L. H. 2000: *Frazil ice formation and incorporation of sediments into sea ice in the Kara Sea*. PhD thesis, Geophysical Institute, University of Bergen.
- Smedsrud, L. H. 2001: Frazil ice entrainment of sediment: large tank laboratory experiments. *J. Glaciol.* 47, 461–471.
- Smedsrud, L. H. 2002: A model for entrainment of sediment into sea ice by aggregation between frazil ice crystals and sediment grains. *J. Glaciol.* 48, 51–61.
- Smedsrud, L. H. & Eicken, H. 2003: *Report on sea-ice data for the KAREX 94 Expedition*. Nor. Polarinst. InternRapp. Ser. 15. Tromsø: Norwegian Polar Institute.
- Svensson, U. & Omstedt, A. 1998: Numerical simulations of frazil ice dynamics in the upper layers of the ocean. *Cold Reg. Sci. Technol.* 28, 29–44.